

Chaos in *pp*-wave spacetimes

Jiří Podolský and Karel Veselý

Department of Theoretical Physics, Faculty of Mathematics and Physics, Charles University, V Holešovičkách 2, 180 00 Prague 8, Czech Republic

(Received 21 May 1998; published 1 September 1998)

We demonstrate the chaotic behavior of timelike, null, and spacelike geodesics in nonhomogeneous vacuum *pp*-wave solutions by analytic and fractal methods. This seems to be the first known example of a chaotic motion in exact radiative spacetime. [S0556-2821(98)50418-3]

PACS number(s): 04.30.-w, 04.20.Jb, 05.45.+b

In the context of general relativity the first system for which a chaotic behavior of solutions to the Einstein equations has been recognized and thoroughly studied were Bianchi type IX cosmological models (see, for example, [1,2], and references therein). Complicated nonlinear effects also occur in systems with coupled gravitational and scalar fields [3–6].

Other types of problems providing nonlinear dynamical systems in general relativity are the studies of geodesic motion in given spacetimes. In particular, the chaotic behavior of geodesics in the relativistic analogue of the two fixed-centers problem (modeled by extreme black holes) was examined in [7–10]. Chaotic geodesic motion was also found in (perturbed) Schwarzschild spacetime [11–14], in some static axisymmetric spacetimes [15,16] and in a topologically nontrivial Robertson-Walker universe [17,18].

Here we investigate motion in exact gravitational waves, namely, in the widely known class of vacuum *pp* waves [19], the metric of which can be written in the form

$$ds^2 = 2d\zeta d\bar{\zeta} - 2dudv - (f + \bar{f})du^2, \tag{1}$$

where $f(u, \zeta)$ is an arbitrary function of u and the complex coordinate ζ spanning the plane wave surfaces $u = \text{const}$. When f is linear in ζ , the metric (1) represents a Minkowski universe. The case $f = g(u)\zeta^2$ describes plane gravitational waves (“homogeneous” *pp* waves) which have thoroughly been investigated (see [19] for references). This simple example of an exact radiative spacetime has also been used for the construction of sandwich and impulsive waves [20,21].

However, here we wish to study geodesics in more general, nonhomogeneous vacuum *pp* waves and demonstrate their chaotic behavior. The geodesic equations for Eq. (1) are

$$\ddot{\zeta} + \frac{1}{2} \bar{f}_{,\bar{\zeta}} U^2 = 0, \tag{2}$$

$$\dot{u} = U = \text{const}, \tag{3}$$

$$\ddot{v} + (f_{,\zeta} \dot{\zeta} + \bar{f}_{,\bar{\zeta}} \dot{\bar{\zeta}}) U + \frac{1}{2} (f + \bar{f})_{,u} U^2 = 0, \tag{4}$$

where the dot denotes $d/d\tau$ with τ being an affine parameter. Assuming also a condition normalizing the four-velocity such that $U_\mu U^\mu = \epsilon$, where $\epsilon = -1, 0, +1$ for timelike, null, or spacelike geodesics, we get

$$\dot{v} = \frac{1}{2} U^{-1} [2\dot{\zeta}\dot{\bar{\zeta}} - (f + \bar{f})U^2 - \epsilon]. \tag{5}$$

We consider $U \neq 0$ [for $U = 0$ Eqs. (2)–(4) can be integrated yielding only some trivial geodesics]. By differentiating Eq. (5) and using Eq. (2) we immediately obtain Eq. (4) which can thus be omitted. Hence it suffices to find solutions of Eq. (2) since $v(\tau)$ can then be obtained by integrating Eq. (5), and $u(\tau) = U\tau + u_0$.

The remaining Eq. (2) has the same form for timelike, null, and spacelike geodesics. Introducing real coordinates x and y by $\zeta = x + iy$ we get a system which, for f independent of u , follows from the Hamiltonian

$$H = \frac{1}{2} (p_x^2 + p_y^2) + V(x, y), \tag{6}$$

where the potential is $V(x, y) = \frac{1}{2} U^2 \text{Re } f$. For nonhomogeneous *pp*-wave spacetimes given by $f = C\zeta^n$, $C = \text{const} > 0$, $n = 3, 4, \dots$, the corresponding potential

$$V(x, y) = \frac{1}{2} C U^2 \text{Re } \zeta^n \tag{7}$$

is called “ n saddle.” It can be visualized in polar coordinates ρ, ϕ where $\zeta = \rho \exp(i\phi)$, in which it takes the form $V(\rho, \phi) = \frac{1}{2} C U^2 \rho^n \cos(n\phi)$.

Now, it was shown previously by Rod, Churchill, and Pecelli in a series of papers [22–25] that motion in the Hamiltonian system (6) with the n -saddle potential (7) is chaotic.

Let us first briefly summarize their results for the simplest case $n = 3$. The corresponding potential (after removing an unimportant multiplicative factor by a suitable rescaling of τ)

$$V(x, y) = \frac{1}{3} x^3 - xy^2 \tag{8}$$

is called a “monkey saddle.” Interestingly, this is a special case of famous Hénon-Heiles Hamiltonian [26] which is known to be a “textbook” example of a chaotic system (however, their quadratic terms are absent in our case). This particular case of the Hénon-Heiles Hamiltonian has been investigated by Rod [22]. He concentrated on bounded orbits in the energy manifolds $H(x, y, p_x, p_y) = E > 0$. The homogeneity of V guarantees that the orbit structure for any two positive values of E is isomorphic modulo a constant scale factor and adjustment of time, $x \rightarrow \tilde{x} = \lambda x$, $y \rightarrow \tilde{y} = \lambda y$ and τ

$\rightarrow \tilde{\tau} = \tau/\sqrt{\lambda}$, results in $E \rightarrow \tilde{E} = \lambda^3 E$. Therefore, without loss of generality one can restrict to one particular value of E .

In order to describe the topological structure of all bounded orbits Rod first constructed three basic *unstable periodic orbits* (denoted by Π_j) which are *isolated invariant sets* for the flow. The region in which these bounded orbits occur can be decomposed into three disjoint cells R_j (see [22] or [27] for details); each contains only one orbit Π_j and no other bounded orbits. Hence, Π_j is the only invariant set in R_j , i.e., it is isolated.

Subsequently, Rod investigated *orbits asymptotic to basic orbits* Π_j as $\tau \rightarrow \pm\infty$ and showed that these asymptotic sets intersect transversely. This gives the existence of orbits that “connect” the orbits Π_j : they are *homoclinic* (asymptotic to the same periodic orbit in both time directions) or *heteroclinic* (asymptotic to two different periodic orbits, one in each time direction). It is the existence of these orbits that illustrates complicated chaotic structure of the flow.

The topology of possible orbits in phase space can also be represented by symbolic dynamics given here by a set of bi-infinite sequences, $s \equiv \dots, s_k, s_{k+1}, s_{k+2}, \dots$, where $s_k \in \{1, 2, 3\}$, $s_k \neq s_{k+1}$. Using a topological version of the Smale horseshoe map, it was shown in [22] that to any bi-infinite sequence of symbols $\{1, 2, 3\}$ there exists an *uncountable number of bounded orbits* running through the blocks R_j in the prescribed order as τ goes from $-\infty$ to $+\infty$. Also, the flow admits at least a countable number of nondegenerate homoclinic and heteroclinic orbits.

Rod remarked that these results could be refined if the unstable periodic orbits Π_j were known to be hyperbolic so that they would admit stable and unstable asymptotic manifolds. Consequently, to each periodic symbol sequence there would correspond a countable collection of *periodic* orbits. The difficulties in proving the hyperbolicity of Π_j were subsequently overcome in [23]. In [24], summarizing and generalizing some previous results [25], the Hamiltonians (6), (8) were presented as examples of a system for which the Smale horseshoe map can *explicitly* be embedded as a subsystem into the flow along the homoclinic and heteroclinic orbits. This completed the proof of chaotic behavior of the studied system.

Similar results hold for geodesic motion in arbitrary non-homogeneous *pp* waves with the structural function of the form $f = C\zeta^n$, where $n \geq 4$, i.e., for a general n -saddle potential (7). It was shown in [22,25] that the decomposition into isolating cells R_j , $j = 1, 2, \dots, n$, each containing exactly one of the basic unstable periodic solutions Π_j , is analogous to the case $n = 3$. Subsequently, the orbits Π_j were proven to be hyperbolic [23] and the existence of homoclinic and heteroclinic orbits was established [24]. Again, given any bi-infinite sequence, uncountably many orbits can be found which pass from one block containing Π_j to the other in the specified order.

In order to independently support these arguments for the chaotic behavior of geodesics in nonhomogeneous *pp* waves we investigate the motion also by a fractal method. Complementary to the analysis described above, we concentrate on *unbounded* geodesics and we do not restrict to the same energy manifold $E = \text{const}$.

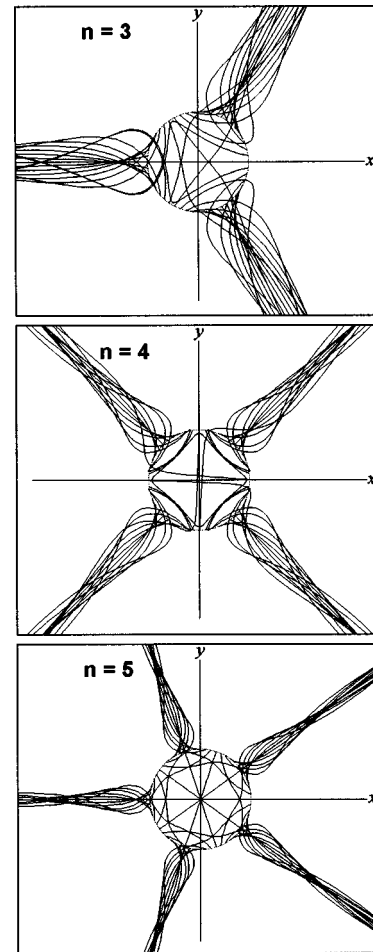


FIG. 1. Geodesics starting from a unit circle escape to infinity only along one of the n channels.

Chaos is usually indicated by a sensitive dependence of the evolution on the choice of initial conditions. The coordinate independent fractal method (see for example [2,7,8,10]) starts with a definition of different asymptotic outcomes (given here by “types of ends” of all possible trajectories). A set of initial conditions is evolved numerically until one of the outcome states is reached. Chaos is uncovered if the basin boundaries that separate initial conditions leading to different outcomes are fractal. Such fractal partitions are the result of chaotic dynamics. As we shall now demonstrate, we observe exactly these structures in the studied system.

We integrate numerically the equations of motion given by Eqs. (6), (7). The initial conditions are chosen such that the geodesics start at $\tau=0$ from a unit circle in the (x, y) plane (because of the homogeneity of the n -saddle potential all other geodesics can simply be obtained by a suitable re-scaling). It is natural to parametrize the initial positions by an angle $\phi \in [-\pi, \pi)$ such that $x(0) = \cos \phi$, $y(0) = \sin \phi$. In Fig. 1 we present typical trajectories of geodesics for $n = 3, 4, 5$, when $\dot{x}(0) = 0 = \dot{y}(0)$. We observe that each unbounded geodesic escapes to infinity (where for $n \geq 3$ the curvature singularity is located) *only along* one of the n channels in the potential. The axes of these outcome channels are given in polar coordinates by the condition

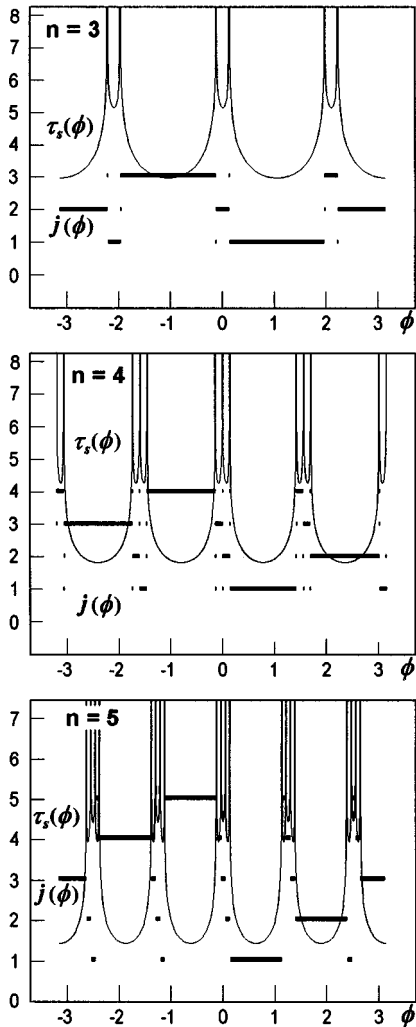


FIG. 2. The functions $j(\phi)$ and $\tau_s(\phi)$ indicate that basin boundaries separating different outcomes are fractal.

$\cos(n\phi_j) = -1$, $j = 1, \dots, n$, and represent radial lines “of steepest descent” since $V \rightarrow -\infty$ as $\rho \rightarrow \infty$ most rapidly along them. (For nonzero initial velocities more geodesics prefer one of the channels but the character of motion does not change significantly [27].)

In fact, any unbounded geodesic oscillates around the radial axis $\phi_j = (2j-1)\pi/n$ of the corresponding j th outcome channel. Introducing $\Delta\phi_j(\tau) = \phi(\tau) - \phi_j$ we find asymptotically that $\rho \approx [(n/2-1)\sqrt{CU^2}(\tau_s - \tau)]^{2/(2-n)}$ as $\rho \rightarrow \infty$ and

$$\Delta\phi_j(\tau) \approx (\tau_s - \tau)^\alpha (A \cos[b \ln(\tau_s - \tau)] + B \sin[b \ln(\tau_s - \tau)]), \quad (9)$$

where $\alpha = \frac{1}{2}(n+2)/(n-2)$, $b = \frac{1}{2}\sqrt{7n^2 - 4n - 4}/(n-2)$, and A, B are constants. As the geodesics approach the singularity at $\rho = \infty$, $\tau \rightarrow \tau_s$, the frequency of their oscillations around ϕ_j grows to infinity while the amplitude of oscillations tends to zero.

Let us return back to our observation that all unbounded geodesics approach infinity through only n distinct channels. These represent possible outcomes of our system and we

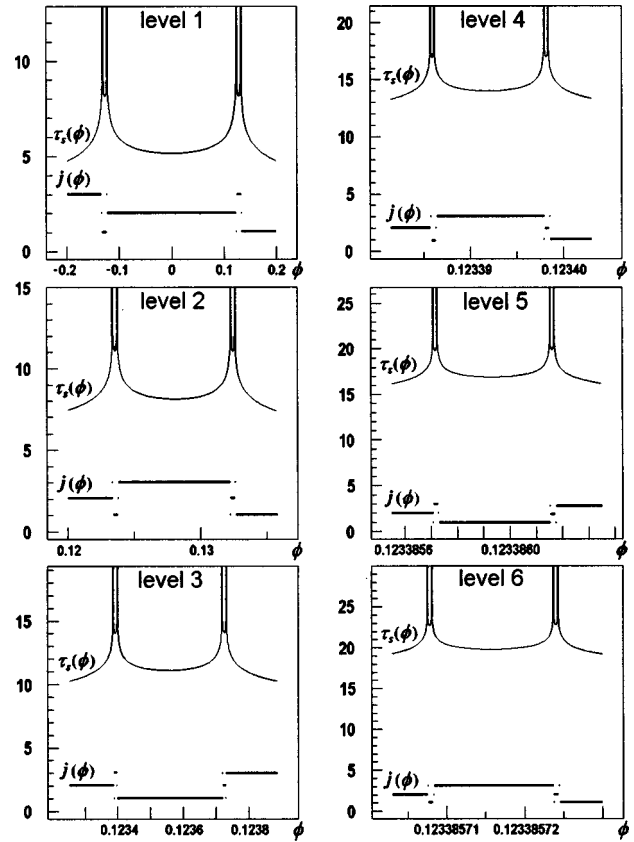


FIG. 3. The fractal structure described by $j(\phi)$ and $\tau_s(\phi)$ is clearly confirmed here by zooming in the interval around $\phi \approx 0$ for $n=3$.

assign them symbol j which takes one of the corresponding values, $j \in \{1, 2, \dots, n\}$ (thus, for example, $j=1$ means that the geodesic approach infinity at $\rho = \infty$ through the first channel with the axis $\phi_1 = \pi/n$ as $\tau \rightarrow \tau_s > 0$). From Fig. 1 we observe that in certain regions the function $j(\phi)$ depends very sensitively on the initial position given by ϕ . We calculated $j(\phi)$ numerically for $n=3, 4, 5$ —the results are shown in Fig. 2. Also, in the same diagrams we plot the function $\tau_s(\phi)$ which takes the value of the parameter τ when the singularity at $\rho = \infty$ is reached by a given geodesic.

Clearly, the boundaries between the outcomes appear to be fractal which can be confirmed on the enlarged detail of the image and the enlarged detail of the detail, etc. In Fig. 3 we show such zooming in of the fractal interval localized around the value $\phi \approx 0$ for $n=3$ (there are two symmetric fractal intervals in this case around $\phi \approx \pm \frac{2}{3}\pi$) up to the sixth level. At each level the structure has the same property, namely, that between two larger connected sets of geodesics with outcome channels j_1 and $j_2 \neq j_1$ there is always a smaller connected set of geodesics with outcome channel j_3 such that $j_3 \neq j_1$ and $j_3 \neq j_2$. Similarly as in [7,10], the structure of the initial conditions resembles three mixed Cantor sets, and this fact is a manifestation of chaos.

The above structure of $j(\phi)$ has its counterpart in the fractal structure of $\tau_s(\phi)$, see Fig. 2 and Fig. 3. We observe that the value of τ_s goes to infinity on each discontinuity of $j(\phi)$, i.e., on any fractal basin boundary between the differ-

ent outcomes. There is an infinite set of peaks corresponding to chaotic bounded orbits which never “decide” on a particular outcome, and so never escape to infinity. The value of τ_s also increases in nonchaotic regions of ϕ as one zooms in the higher levels of the fractal. This is natural since these levels are given by geodesics which undergo “more bounces” on the potential walls before falling into one of the outcome channels so that their values of τ_s are greater.

We demonstrated chaotic behavior of geodesics in nonhomogeneous pp waves by invariant analytic and numerical

methods. As far as we know, this is the first explicit demonstration of chaos in *exact* radiative spacetimes (chaotic interaction of particles with linearized gravitational waves on given backgrounds has already been studied in [11,13,28–30]). Since pp -wave solutions are the simplest gravitational waves it would be an interesting task to search for a chaotic motion in other radiative spacetimes.

We acknowledge the support of Grant No. GACR-202/96/0206 and Grant No. GAUK-230/1996.

-
- [1] *Deterministic Chaos in General Relativity*, edited by D. Hobill, A. Burd, and A. Coley (Plenum, New York, 1994).
- [2] N. J. Cornish and J. J. Levin, Phys. Rev. Lett. **78**, 998 (1997); Phys. Rev. D **55**, 7489 (1997).
- [3] M. W. Choptuik, Phys. Rev. Lett. **70**, 9 (1993).
- [4] E. Calzetta and C. El Hasi, Class. Quantum Grav. **10**, 1825 (1993).
- [5] S. Blanco, A. Costa, and O. A. Rosso, Gen. Relativ. Gravit. **27**, 1295 (1995).
- [6] N. J. Cornish and J. J. Levin, Phys. Rev. D **53**, 3022 (1996).
- [7] G. Contopoulos, Proc. R. Soc. London **A431**, 183 (1990); **A435**, 551 (1991).
- [8] C. P. Dettmann, N. E. Frankel, and N. J. Cornish, Phys. Rev. D **50**, R618 (1994).
- [9] U. Yurtsever, Phys. Rev. D **52**, 3176 (1995).
- [10] N. J. Cornish and G. W. Gibbons, Class. Quantum Grav. **14**, 1865 (1997).
- [11] L. Bombelli and E. Calzetta, Class. Quantum Grav. **9**, 2573 (1992).
- [12] W. M. Vieira and P. S. Letelier, Phys. Rev. Lett. **76**, 1409 (1996).
- [13] P. S. Letelier and W. M. Vieira, Class. Quantum Grav. **14**, 1249 (1997).
- [14] S. Suzuki and K. Maeda, Phys. Rev. D **55**, 4848 (1997).
- [15] V. Karas and D. Vokrouhlický, Gen. Relativ. Gravit. **24**, 729 (1992).
- [16] Y. Sota, S. Suzuki, and K. Maeda, Class. Quantum Grav. **13**, 1241 (1996).
- [17] C. M. Lockhart, B. Misra, and I. Prigogine, Phys. Rev. D **25**, 921 (1982).
- [18] R. Tomaschitz, J. Math. Phys. **32**, 2571 (1991).
- [19] D. Kramer, H. Stephani, M. A. H. MacCallum, and E. Herlt, *Exact Solutions of Einstein's Field Equations* (Cambridge University Press, Cambridge, England, 1980).
- [20] H. Bondi, F. Pirani, and I. Robinson, Proc. R. Soc. London **A251**, 519 (1959).
- [21] R. Penrose, in *General Relativity*, edited by L. O’Raifeartaigh (Clarendon, Oxford, 1972).
- [22] D. L. Rod, J. Diff. Eqns. **14**, 129 (1973).
- [23] D. L. Rod, G. Pecelli, and R. C. Churchill, J. Diff. Eqns. **24**, 329 (1977).
- [24] R. C. Churchill and D. L. Rod, J. Diff. Eqns. **37**, 23 (1980).
- [25] R. C. Churchill and D. L. Rod, J. Diff. Eqns. **21**, 39 (1976); **21**, 66 (1976).
- [26] M. Hénon and C. Heiles, Astron. J. **69**, 73 (1964).
- [27] J. Podolský and K. Veselý (in preparation).
- [28] H. Varvoglis and D. Papadopoulos, Astron. Astrophys. **261**, 664 (1992).
- [29] C. Chicone, B. Mashhoon, and D. G. Retzliff, Class. Quantum Grav. **14**, 699 (1997).
- [30] F. Kokubun, Phys. Rev. D **57**, 2610 (1998).